

Inhibition of TC-83 Alphavirus by Small Molecule Saracatinib and Piscidin Peptide
Candidates

A Thesis submitted in partial fulfillment of the requirements for the degree of Master of
Science at George Mason University

by

Leykie I. Green
Bachelor of Science
James Madison University, 2022

Director: Aarthi Narayanan, Professor
College of Science

Spring Semester 2024
George Mason University
Fairfax, VA

Copyright 2024 Leykie I. Green
All Rights Reserved

DEDICATION

I dedicate this work to my loving parents who fully supported me in every step of graduate school and life.

TABLE OF CONTENTS

	Page
List of Figures	v
List of Abbreviations	vi
Abstract	vii
Introduction.....	1
Hypothesis.....	5
Aims	6
Methods and Materials.....	7
Anticipated Outcomes.....	10
Results.....	11
Conclusions and Future Studies.....	23
References.....	25

LIST OF FIGURES

Figure	Page
Figure 1.....	12
Figure 2.....	14
Figure 3.....	16
Figure 4.....	18
Figure 5.....	19
Figure 6.....	20
Figure 7.....	22

LIST OF ABBREVIATIONS

Venezuelan Equine Encephalitis Virus.....	VEEV
Central nervous system.....	CNS
Antimicrobial peptides.....	AMPs
Blood-brain barrier.....	BBB
Human brain microvascular endothelial cells.....	HBMEC
Eagle's Minimum Essential Medium	EMEM
Dulbecco's Modified Eagle Medium.....	DMEM
Adenosine triphosphate.....	ATP
Dimethyl sulfoxide.....	DMSO
Cytotoxic concentration.....	CC50
Inhibitory concentration.....	IC50
Multiplicity of infection.....	MOI
Relative luminescence unit.....	RLU

ABSTRACT

INHIBITION OF TC-83 ALPHAVIRUS BY SMALL MOLECULE SARACATINIB AND PISCIDIN PEPTIDE CANDIDATES

Leykie I. Green, M.S.

George Mason University, 2024

Thesis Director: Dr. Aarthi Narayanan

Venezuelan Equine Encephalitis Virus (VEEV) is an encephalitic alphavirus that is known to cause disease in the central nervous system (CNS). It is naturally transmitted by infected mosquitoes and causes disease in equines and humans on a regular basis in various parts of the world. VEEV also has the potential to be aerosolized, and when infection is acquired via the respiratory route, the chances of CNS penetration are higher, with increased incidences of morbidity and mortality. Even if infected individuals clear the infection, there is a potential for long term neurological sequelae in survivors, thus increasing the disease burden. There are currently no FDA-approved therapeutic intervention strategies to treat the encephalitic manifestations of VEEV infection-induced disease. This thesis project focused on establishing early stage efficacy measurements for a candidate small molecule inhibitor, Saracatinib, which is already FDA-approved for the treatment of cancer. In addition, this project also involved screening a small library of

synthetic antimicrobial peptides (AMPs) derived from a parent piscidin peptide. Piscidins are fish-derived, naturally occurring AMPs that have been demonstrated to have antibacterial and immunomodulatory properties. My project was based on the hypothesis that Saracatinib and synthetic piscidin-derived AMPs will demonstrate antiviral activities against VEEV. This project was performed using the attenuated TC-83 strain of VEEV, in the context of several human-derived cell lines of the blood brain barrier (BBB). Analysis of antiviral activities of Saracatinib in the nontoxic range demonstrated that endothelial cells were highly responsive to treatment and showed significant reduction in viral load in treated cells. Screening of the synthetic piscidin library has identified four candidates that showed a statistically significant reduction in viral load in a human astrocyte cell line. Cumulatively, these data provide the foundation for further development of Saracatinib and prioritized synthetic piscidin AMPs as therapeutic intervention strategies against VEEV infection.

INTRODUCTION

Venezuelan equine encephalitis virus (VEEV) as a re-emerging priority pathogen:

Venezuelan equine encephalitis virus (VEEV) is a new world alphavirus that causes disease in humans, in addition to horses, donkeys and mules, thus posing a significant One Health concern (1-3). In cases of naturally acquired infections, mosquitos infected with the virus transmit them to another uninfected species when they bite. VEEV infection is known to cause sporadic cases mostly in Latin America, especially during heavy rainfall. In addition to being transmitted by mosquitoes, VEEV can also be infectious as an aerosol (4, 5). In both routes of infection, VEEV shows tropism towards the central nervous system (CNS) resulting in localized infections in the brain, and damage to the CNS tissue, including the blood brain barrier (BBB). Even in the case of individuals who clear the acute infection, there is potential for long term neurological sequelae thus greatly increasing the disease burden (6, 7). There is currently no FDA-approved therapeutic strategy available to treat VEEV infection. The TC-83 strain of VEEV which is used in this project is a live attenuated strain of virulent VEEV which was previously used to vaccinate at-risk personnel (8). But due to high incidences of adverse events, TC-83 is no longer used as a vaccine candidate. This lack of therapeutic and vaccine approaches to treat VEEV infection poses a major global One Health

challenge, and requires investigation into diverse approaches to arrive at therapeutic solutions.

The cellular composition of the human BBB:

This project places emphasis on the cellular components of the human BBB as the BBB is known to be disrupted in VEEV infections (9-12). The cells of importance at the BBB with reference to VEEV infection are pericytes, microglia, brain endothelial cells, and astrocytes (13). The endothelial cells coat the interior lining of the blood vessels that form the BBB and are responsible for regulating bidirectional transport of critical components including oxygen and nutrients to and from the brain (14, 15). Pericytes are located on top of endothelial cells and are believed to help in angiogenesis and neuronal stabilization for activity (15). This is because they are modulators of capillary diameter and blood flow. These cells are also responsible for controlling the blood pressure near the brain and regulating the permeability in the BBB. SVG p.12 are astrocytes, which are reported to contribute to the maintenance of structural integrity of the BBB as they communicate with both the endothelial cells and the pericytes (14, 15). They have barrier properties since they ensheath most of the brain's microvasculature and they also play a role in what enters and exits via the BBB. Human microglial cells, clone 3, also known as HMC3s, are known to originate from the immune system. They play a pivotal role in the microenvironment for the BBB by initiating inflammation if there is an infection, trauma, or cellular malfunction. For the purposes of this project, these four cell types will be employed, to evaluate the efficacy of prioritized therapeutic options, as determined by changes to viral load in the context of infection.

Small molecule and peptide-based strategies as potential therapeutic options:

Evidence available in the literature based on publications from our laboratory and several colleagues in the field have demonstrated the antiviral potential of multiple small molecules, antimicrobial peptides (AMPs), and antibodies in *in vitro* and *in vivo* VEEV infection models (16-22). In this project, we focused on the small molecule Saracatinib ($C_{27}H_{32}ClN_5O_5$) to assess its ability to inhibit VEEV viral load in different cell types of the human BBB. Saracatinib, a *src* pathway inhibitor, is already FDA approved for the treatment of pulmonary fibrosis, thus making it an ideal candidate for repurposing to treat VEEV infections (23). Fortuitously, during an independent kinome screen performed for other small molecules, our laboratory identified Saracatinib as being potentially capable of altering several signaling pathways that may be critical for VEEV infection. This prompted us to specifically query Saracatinib for antiviral properties against VEEV, using the TC-83 strain.

Our laboratory has previously published that synthetic AMPs derived from naturally occurring AMPs have the potential to inhibit VEEV in multiple cell culture models (24). Therefore, we were interested to assess if Piscidin peptide-derived synthetic AMPs will also be potential candidates to develop as therapeutic options for the treatment of VEEV infection. The lead piscidin peptide which was used as the guide for the design of the synthetic derivatives was derived from the mast cells of Striped Bass. Naturally occurring Piscidin peptides are believed to have antimicrobial and immunomodulatory

properties (25-30). It is believed that their mechanism of action is the toroidal pore formation where the peptide permeabilizes the membrane of the cell and disrupts the membrane, therefore killing the microorganism. In the context of antibacterial outcomes, the peptide's positive charge initially allows it to bind to the negatively charged bacterial surface. Then the amphipathic traits allow them to survive in both hydrophilic and hydrophobic environments, therefore allowing the peptide to create pores on the bacterial cell membrane. In this project, 33 synthetic piscidin AMP derivatives will be assessed for their potential to inhibit VEEV TC-83 infection in astrocytes and thus position prioritized candidates for further development as therapeutic options to treat VEEV infection.

HYPOTHESIS

This project will address two distinct hypotheses:

1. I hypothesize that Saracatinib will elicit an inhibitory effect on the TC-83 strain of VEEV in the nontoxic range, in a cell type independent manner. The inhibitory effect will correlate with lower viral titer as evaluated by an independent assay (plaque assay).
2. I hypothesize that the initial library of AMPs will yield viable peptide candidates that will be successful in decreasing VEEV TC-83 load in a dose dependent manner in the context of an infected cell line. I anticipate that the primary screen will yield viable peptide candidates that can be subjected to independent preclinical development as therapeutic options to treat VEEV infection.

AIMS

Aim 1: To determine the cell type independent therapeutic potential of Saracatinib in reducing TC-83 viral load in multiple cell types relevant to the central nervous system.

1a: To determine concentration-dependent cytotoxicity of Saracatinib in human-based astrocyte, microglia, pericyte, and brain microvascular endothelial cell lines.

1b: To independently validate the inhibitory potential of Saracatinib in the candidate cell lines by performing plaque assay of culture supernatants.

Aim 2: To down select synthetic piscidin AMPs that are able to inhibit VEEV TC-83 virus in one cell type that is relevant to the central nervous system.

2a: To conduct a broad tolerance assessment for all peptides in the synthetic peptide library in the context of astrocytes and identify tolerance ranges for each peptide that can produce nontoxic outcomes.

2b: To perform luciferase assay to down select synthetic piscidins that can elicit an inhibitory effect on VEEV TC-83 in the astrocyte cell line, in the well tolerated range, followed by a plaque assay of culture supernatants.

2c: To perform in-depth cytotoxicity assessments for the down selected peptides and independently verify inhibition of VEEV TC-83.

METHODS AND MATERIALS

Cells and Virus:

The cell lines and the VEEV TC-83 virus that will be employed in the studies included in this project have been previously described in publications from our laboratory (13, 16, 18-21). As such, the methodologies described in those publications will be followed. The cell lines included in this effort are microglial cells (HMC3), African green monkey cells (vero), pericyte cells, astrocyte cells (SVG p.12), and human brain microvascular endothelial cells (HBMEC). The HMC3, SVG p.12, and pericyte cell lines will be maintained in Eagle's Minimum Essential Medium (EMEM), fetal bovine serum, penicillin and streptomycin as an antibiotic, and L-glutamate. The endothelial cells will be maintained in EGM2, supplemented with ascorbic acid, hEGF, GA-1000, hydrocortisone, hFGF-B, VEGF, HEPARIN, and R3-IGF-1. Vero cells will be maintained in Dulbecco's Modified Eagle Medium (DMEM) with fetal bovine serum, penicillin and streptomycin as an antibiotic, and L-glutamate. All cell lines will be maintained at 37°C and 5% CO₂.

Inhibitors, Toxicity Assay/CC50 determination

Saracatinib was obtained from SelleckChem. Most of the piscidin peptides were synthesized by GenScript, while a handful of peptides are from ChinaPeptides. Cell cytotoxicity in the presence of inhibitors will be assessed as previously described (13, 16, 18-21). Briefly, the cells will be treated with the appropriate inhibitor for 18 or 24 hours and Cell Titer Glo will be used to measure the adenosine triphosphate (ATP) levels. The

desired concentrations of the Saracatinib, Piscidin peptide, or dimethyl sulfoxide (DMSO) will be added to the media under the appropriate conditions (pretreatment, co-treatment and post treatment). The regular culture media will be removed from the cells and replaced with drug-containing media for 18 or 24 hours. After the indicated hours, the media will be removed and cell titer glo assay performed (Promega).

Drug Treatment for viral inhibition assessment.

The drug treatments will be carried out as previously described (13, 16, 18-21). The pre-treatment will be carried out at determined concentrations for 1 hour prior to infection. The cells will be infected with the TC-83 virus for one hour following published protocols. Saracatinib will receive the TC-83 virus independent of the drug while the peptides will be mixed with a Luciferase-tagged virus during infection (co-treatment). After the hour, the treatment or co-treatment will be removed and the post-treatment (drug containing media) will be delivered directly and maintained until the desired time when luciferase readout should be made. The supernatants will be collected and frozen until required for the assay.

Luciferase Nano Glo Assay & Bradford Assay

Published methodologies will be followed for these assays (13, 16, 18-21). Briefly, the cells were lysed with 1X lysis buffer. After ensuring that the cells were lysed, 50 μ L of the lysate were transferred to a 96-well plate for the Bradford Assay. For the Nano Glo Assay, the Luciferase buffer and vial substrate were mixed according to the amount needed and 50 μ L was placed in each well. The mixture was left for three minutes

to interact with the Luciferase-tagged viral particles, and then the plate was covered with a protective film after which luciferase activity was measured (Promega).

Plaque Assay

Plaque assays were performed following published protocols (13, 16, 18-21). Vero cells plated in a 12-well format were used. Serially diluted supernatant samples were used to infect confluent vero cell monolayers. After two days, 1mL of 10% paraformaldehyde will be placed in each well for at least one hour and then the plaque plugs will then be deplugged carefully. The wells will then be stained with Crystal violet for at least fifteen minutes and then gently rinsed off with tap water and plaques were counted.

Statistical Analysis

All experiments were performed as triplicate samples. Data processing was performed using the GraphPrism software and student T test was used for statistical analyses.

ANTICIPATED OUTCOMES

In the end, it is expected that the antiviral properties of Saracatinib and the Piscidin peptides will be better understood. There may be varying levels of viral inhibition since a couple of cell lines will be used for the Saracatinib portion with many concentrations. On the other hand, the Piscidin peptides may also vary since thirty-three peptides will be used at different concentrations.

RESULTS

Cell type independent inhibition of VEEV TC-83 by Saracatinib.

To address Aim 1, the experiments focused on Saracatinib treatment of astrocytes (SVG.p12), pericytes, HMC3, and HBMEC cells and the impact of the treatment on TC-83 replication in the treated cells. To that end, as a first step, the cytotoxic concentration 50 (CC50) value of Saracatinib in each of the above-mentioned cell lines was calculated. The CC50 value was determined in the form of an 8-point dilution curve with the maximum concentration of Saracatinib that was tested was 200 μM . The cells were treated with either DMSO (negative control) or increasing concentrations of Saracatinib in a 96-well format for 24h after which the survival of the cells was measured by Cell Titer Glo assay. The outcomes of the assay are indicated in Figure 1. The HMC3 cells had a CC50 value of 49.93 μM , the SVG p.12 cells had a CC50 value of 30.97 μM , the pericytes cells had a CC50 value of 30.74 μM , and the endothelial cells had a CC50 value of 52.39 μM .

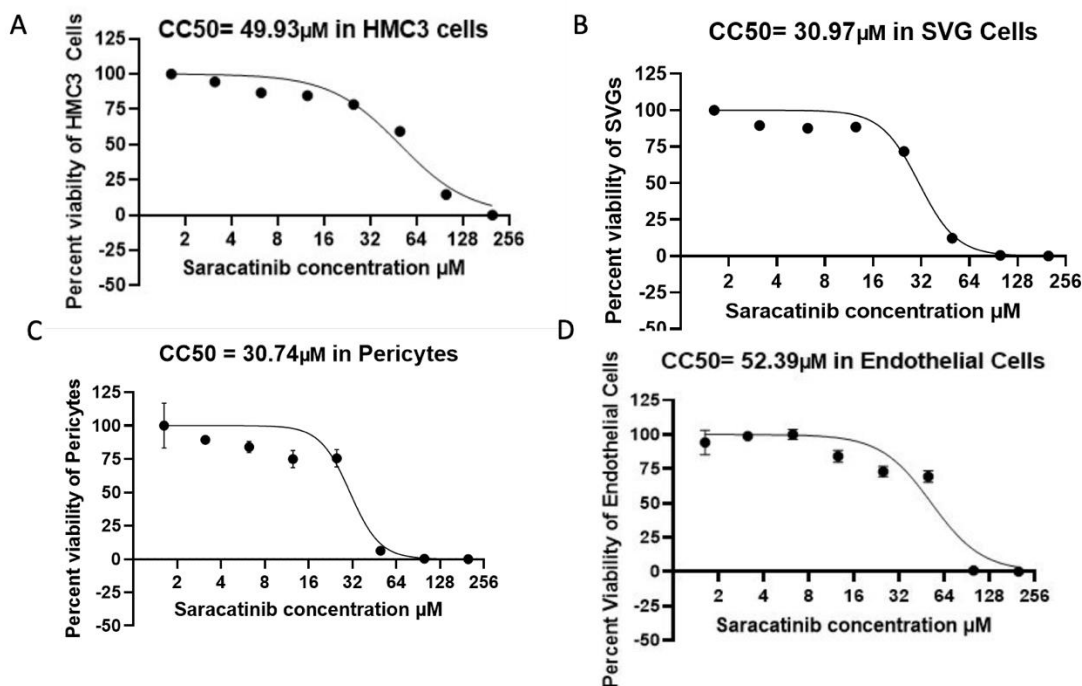


Figure 1: The CC50 values for Saracatinib in the context of (A) HMC3s that gave a CC50 of 49.93 μM, (B) SVG p.12 that gave a CC50 of 30.97 μM, (C) pericytes that produced a CC50 of 30.74 μM, and (D) endothelial cells that gave a CC50 of 52.39 μM. All four cell lines were treated with Saracatinib for 24 hours and then the ATP activity was measured with Cell Titer Glo at the 24-hour mark to detect changes in cell viability. The data was processed using GraphPrism.

Following the determination of the CC50 values, the inhibitory potential of saracatinib calculated in the form of half-maximal inhibitory concentration (IC50) was assessed on the same four cell lines. They were pretreated with Saracatinib at 50 μM, 25 μM, 10 μM, 5 μM, and 1 μM for 1 hour individually. After the hour, the cells were infected with TC-83 for 1 hour at a multiplicity of infection (MOI) of 0.1. Following the 1h infection timeframe, the cells were post-treated with Saracatinib at 50 μM, 25 μM, 10 μM, 5 μM, and 1 μM. Twenty three hours later, the supernatants were collected to

quantify the extracellular viral titer of TC-83 by plaque assay. The outcomes of the IC₅₀ study are shown in Figure 2. The 50 μ M concentration of the drug in the HMC3 cell line demonstrated an approximate a 3-log difference compared to the DMSO, a log difference for both 25 μ M and 10 μ M. Not much of an impact on viral multiplication was observed at the 5 μ M and 1 μ M concentrations (Figure 2A). The 50 μ M concentration in the context of SVG p.12 cells had a 1-log decrease, and no difference in the remaining four concentrations (Figure 2B). Pericytes had about a 2 ½- log decrease at the 50 μ M concentration, and roughly a 1-log decrease in the 25 μ M concentration, whereas the 10 μ M, 5 μ M, and 1 μ M concentrations did not demonstrate any significant inhibitory effect (Figure 2C). Lastly, the HBMECs demonstrated consistent inhibition in all four concentrations tested (Figure 2D). Specifically, the 50 μ M has roughly a 4-log decrease, the 25 μ M, and 5 μ M have a 2 ½ -log decrease, while the 10 μ M and 1 μ M have about a 2-log decrease compared to the DMSO (Figure 2D). Cumulatively, the IC₅₀ dataset demonstrates that Saracatinib elicited varying levels of viral inhibition in all four central nervous system relevant cell types tested, thus adding support to the hypothesis that Saracatinib will exert an inhibitory effect on VEEV TC-83 in a cell type independent manner.

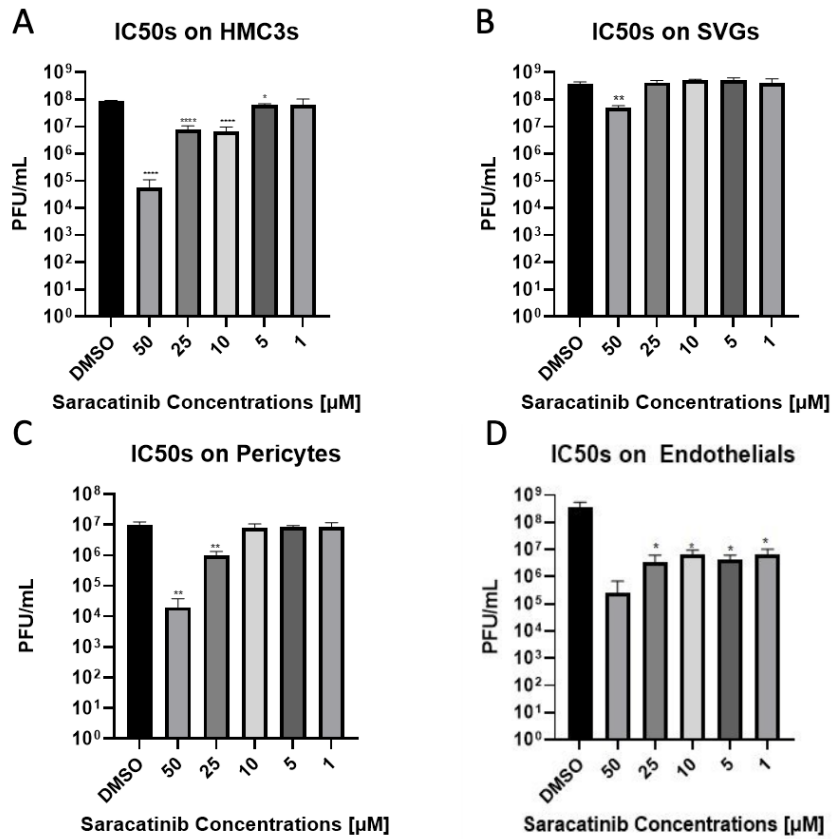


Figure 2: The IC50 values for Saracatinib in the context of VEEV TC-83 infected HMC3s (A), SVG p.12 (B), pericytes (C), and endothelial (D) cells. All four cell lines were pretreated for 1h, infected with TC-83 (MOI: 0.1), and post-treated for 23h. The supernatants were analyzed by plaque assay to quantify viral load. Triplicate datasets were processed on GraphPad and T-test was performed to calculate significance.

Screening of the synthetic piscidin AMP library for candidates with inhibitory potential against VEEV TC-83.

As a first step, gross tolerance of the SVG.p12 astrocyte cell line to increasing concentrations of the piscidin peptides was determined by measuring cellular tolerance for up to 24h. The approach was similar to the cytotoxicity assessment as described for Saracatinib. For the gross tolerance assessment, the astrocytes were plated in a 96-well format, treated with three concentrations of each peptide (100 µg/mL, 50 µg/mL, and 25 µg/mL), and the treated cells assessed for viability by Cell Titer Glo assay after twenty four hours. Of the 33 peptides analyzed, the highest concentration tested was in many cases less tolerated by the cells, with viability dropping by >75%. Several peptides were somewhat tolerated by the cells at the intermediate concentration, while the lowest concentration tested appeared to be mostly well tolerated by the cells with the survival being greater than 80%. The gross tolerance assessment data are shown in Figure 3.

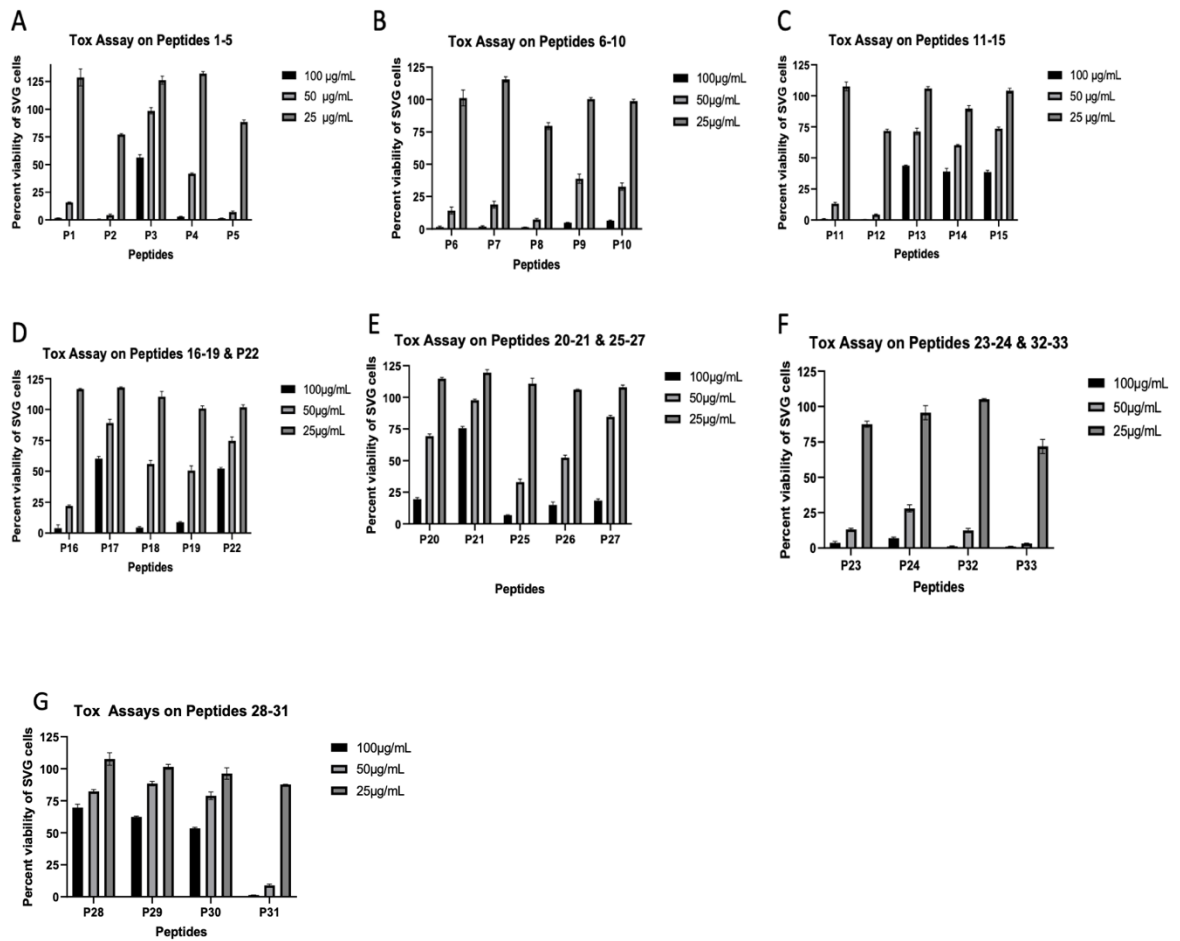


Figure 3: Gross tolerance of SVG p.12 to the synthetic piscidin peptides as determined at three increasing concentrations. The SVG p.12 cells were treated for 24 hours with the indicated peptide and then the ATP activity was measured with Cell Titer Glo at the 24-hour mark.

Following the tolerance assessments, the impact of peptide treatment on VEEV TC-83 in infected astrocytes were determined. To perform the efficacy assessments, a co-treatment strategy was employed in addition to the pre- and the post-treatment stages. During the co-treatment stage, the peptide was present in the viral inoculum. Twenty-four peptides were chosen for 25 μ g/mL concentration of peptide, five peptides were chosen for 10 μ g/mL concentration of peptide, and four peptides were chosen for 50 μ g/mL concentration (Figure 4). P1, P4, P5, P6, and P18 showed the most Relative Luminance Unit (RLU) reduction compared to the DMSO, while P27, P28, and P30 showed the least fluorescence reduction (Figure 4A, B). The 0 μ g/mL had to be repeated due to a missing peptide, P29, and to verify the RLU for P21. P12 had little to no reduction compared to the DMSO, while P2 and P8 gave about a log reduction in Figure 4C. P31 and P33 had a 2 1/2-log reduction compared to DMSO (Figure 4C). P3 had a three-log difference compared to the DMSO and P17 had a little over a two-log difference compared to the DMSO as well (Figure 4D). P21 and P29 did not inhibit viral growth in this experiment since it is similar to DMSO (Figure 4E).

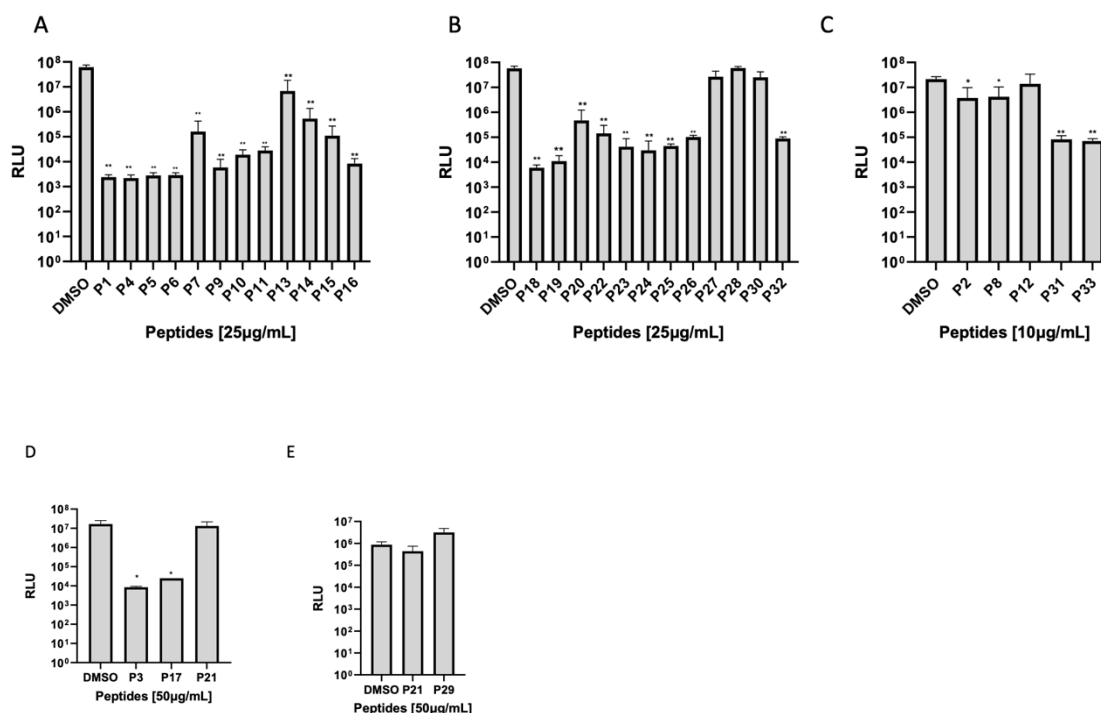


Figure 4: TC-83 viral load in infected astrocytes following peptide treatment as determined by luciferase quantification assay. Above are data shown for 25µg/mL, 50µg/mL, and 10µg/mL for the indicated peptides. The Luciferase results were divided by the Bradford results well by well. Each graph represents one 96-well plate. (A,B) Twenty-four peptides were chosen for 25µg/mL concentration. (C) Five peptides were best for 10µg/mL, and (D,E) four peptides were selected for 50µg/mL.

Careful analysis of data shown in Figure 4 allowed us to down select four peptides, P1, P4, P5, and P6 for more in-depth assessment of cellular tolerance in the form of the 8-point concentration CC50 assessment as previously described for Saracatinib. P1 produced a CC50 of 33.19 µg/mL. P4 gave a CC50 of 38.01 µg/mL. P5 gave a CC50 of 39.36 µg/mL. Lastly, P6 gave a CC50 of 42.23 µg/mL. The plot near 12µg/mL in P5 (Figure 5B) is higher than the calculated slope because there was an inconsistency with one of the DMSO wells. One of the samples produced a cell viability

that was higher than the other two samples, causing the data set for the DMSO at that concentration to have higher cell viability than the calculated amount (Fig5C). In addition, P4, P5, and P6 developed a CC50 close in range due to the fact that they are derivatives of the same peptide. Therefore, it can be inferred that they had similar mutations.

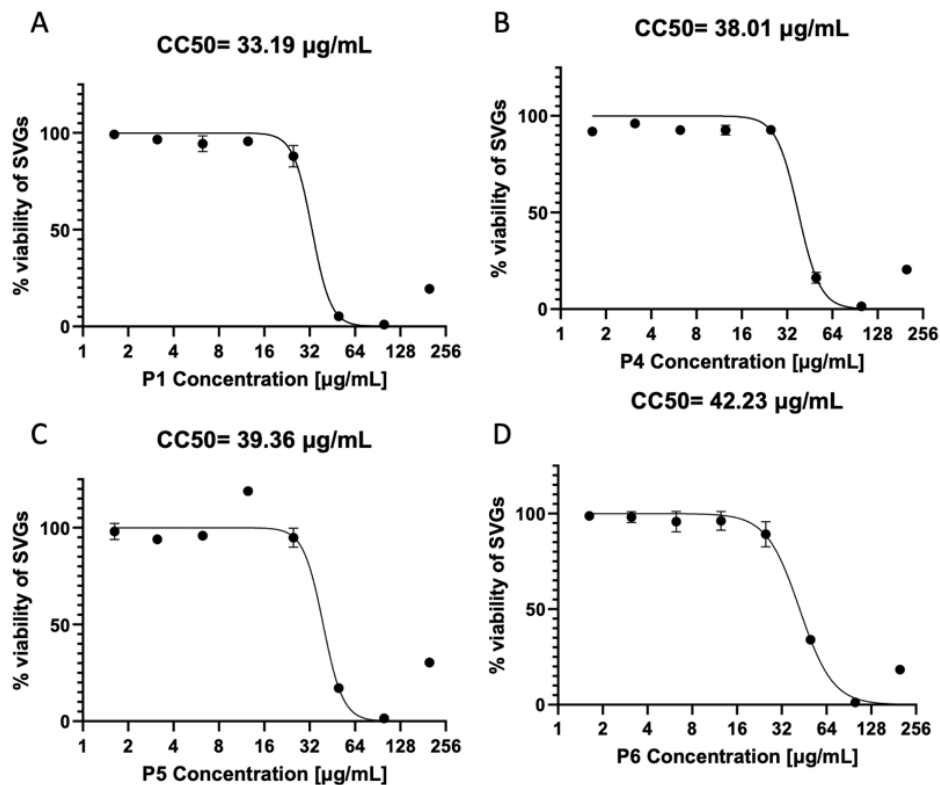


Figure 5: CC50 values for the four candidates: P1, P4, P5, & P6 in astrocyte cells: A) P1 produced a CC50 of 33.19 $\mu\text{g/mL}$. B) P4 gave a CC50 of 38.01 $\mu\text{g/mL}$. C) P5 gave a CC50 of 39.36 $\mu\text{g/mL}$. D) P6 gave a CC50 of 42.23 $\mu\text{g/mL}$. Peptides P4, P5, and P6 are all derivatives of P1 resulting in CC50 values close in range.

As a next step, we performed inhibitory potential assessment for the four down selected peptides, P1, P4, P5, and P6 to address whether the inhibition shows dose dependency. To that end, the infected astrocytes were treated with each peptide at either a high concentration (25 $\mu\text{g}/\text{mL}$) or a low concentration (10 $\mu\text{g}/\text{mL}$), and viral load quantified by luciferase assay. The outcomes of the dose dependency study are shown in Figure 6. At the higher concentration tested, the data indicate that P1 and P4 show a 4-log reduction in Figure 6A. P5 and P6 have a 3 $\frac{1}{2}$ and a 3-log reduction respectively. On the other hand, the 10 $\mu\text{g}/\text{mL}$ demonstrated less viral inhibition. P1 showed about $\frac{1}{2}$ log reduction, both P4 and P5 showed no inhibition, and P6 showed the highest amount of inhibition with a 1-log reduction (Figure 6B). Cumulatively, the data in Figure 6 show that the four down selected peptides show dose dependent inhibition of VEEV TC-83.

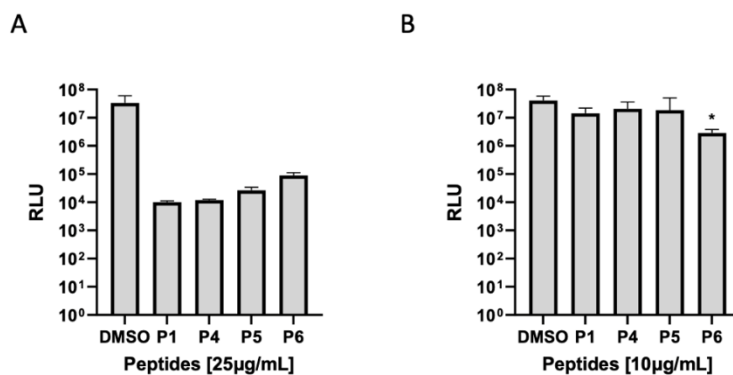


Figure 6: Luciferase assay based assessment of dose-dependent viral inhibition by down selected piscidin AMPs. A) P1 and P4 had approximately a 3 $\frac{1}{2}$ log reduction in RLU, P5 had about a 3-log reduction and P6 had about a 2 $\frac{1}{2}$ log reduction in RLU. B) P1 demonstrates at most half a log reduction in RLU, while P4 and P5 pose no viral reduction in RLU compared to DMSO, and P6 demonstrates roughly a log reduction in RLU compared to DMSO.

As a final step, we performed quantification of extracellular virus titer by plaque assay for the same four peptides under the same conditions as described for the luciferase assay (data shown in Figure 6). This step was performed to differentiate between the intracellular virus (which is measured by the luciferase assay) and the extracellular viral load (which is measured by the plaque assay). The plaque assay outcomes at 25 μ g/mL (Figure 7A) and 10 μ g/mL (Figure 7B, C) are shown in Figure 7. Treatment with the four candidate peptides at 25 μ g/mL resulted in no detectable plaques, suggesting that there was robust inhibition of the extracellular virus. At the lower concentration tested, P1 gave about 1/2 log reduction, P4 and P5 produced no inhibition compared to the DMSO, and P6 gave about 1 1/2 log reduction (Figure 7 B). P5 and P6 were replaques due to potential inconsistencies in the first round of experiments. Figure 7C demonstrates the outcomes of the repeated assay. P5 did not show any inhibition and P6 had about 1 1/3- log reduction. Overall, there is a correlation between the intracellular and extracellular viral loads for the four prioritized piscidin synthetic peptides. The outcomes of these studies were able to successfully down select four piscidin synthetic AMPs that can be subsequently positioned for in-depth preclinical studies as an inhibitory strategy for VEEV.

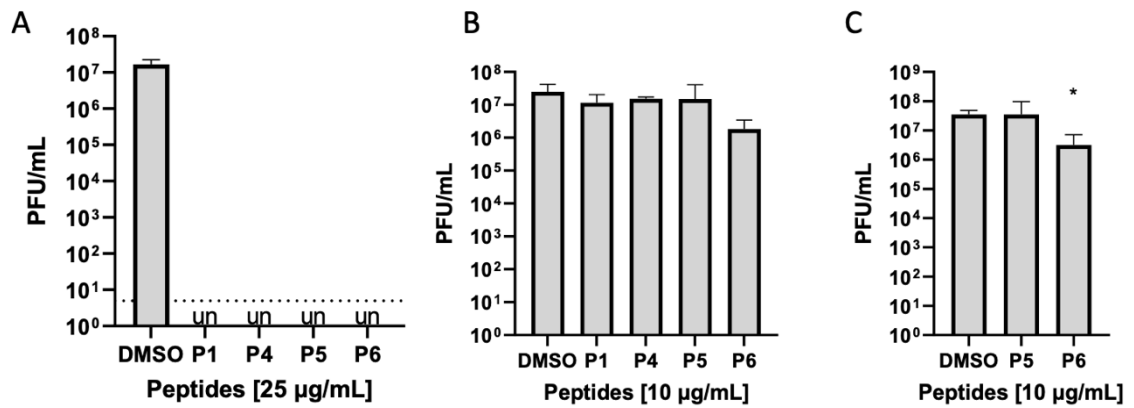


Figure 7: Plaque assays of the four peptide candidates at 25µg/mL and 10µg/mL. (A) At the higher concentration tested, no detectable plaques were observed for P1, P4, P5, and P6. (B) At the lower concentration of peptides, P1, P4, and P5 did not result in any significant decrease in viral titer while P6 demonstrated roughly 1 log difference compared to the DMSO.

CONCLUSIONS AND FUTURE STUDIES

The data collected by the experiments described in the results section support the hypotheses that were put forward for Saracatinib and the piscidin synthetic peptides. Specifically, in the context of Saracatinib, a cell type independent inhibition of VEEV TC-83 was observed in the four central nervous system related cell lines that were tested. Interestingly, the endothelial cells showed the best response to Saracatinib inhibition while the SVGs were the least responsive. The various cell types also demonstrated different cytotoxicity profiles to Saracatinib, which will need to be taken into consideration in any further preclinical assessments as a treatment strategy against VEEV.

Thirty three synthetic piscidin peptides were evaluated for any potential to inhibit VEEV TC-83 in the context of astrocytes. Our data show that several peptide candidates show the potential to inhibit TC-83, but four candidates emerged as priorities. P1, P4, P5, and P6 showed dose dependent inhibition of VEEV TC-83 without eliciting too significant toxicity to the cells.

Moving forward, Saracatinib will need to be assessed in depth for its potential to interrupt viral life cycle in infected cells, and potentially inhibit inflammatory outcomes in the astrocyte and the microglial cells. Given the high responsiveness of the endothelial cells to Saracatinib, it will also be interesting to determine if the treatment strategy can preserve endothelial integrity at the blood brain barrier in the context of VEEV infection. In the context of the synthetic piscidins, the impact of the AMPs in the context of other

cell types will need to be assessed. Importantly, an interesting perspective will also be to ascertain which specific stage of the viral life cycle is inhibited the peptides. Pending a thorough investigation of the in vitro aspects for Saracatinib and the down selected piscidin synthetic AMPs, in vivo efficacy will have to be determined in appropriate models of VEEV infection.

REFERENCES

1. Guzmán-Terán C, Calderón-Rangel A, Rodríguez-Morales A, Mattar S. “Venezuelan equine encephalitis virus: the problem is not over for tropical America.” *Ann Clin Microbiol Antimicrob*. 2020;19(1):19. Published 2020 May 19. doi:10.1186/s12941-020-00360-4
2. Interactions of Equine Viruses with the Host Kinase Machinery and Implications for One Health and Human Disease. Anderson C, Baha H, Boghdeh N, Barrera M, Alem F, Narayanan A. *Viruses*. 2023 May 13;15(5):1163. doi: 10.3390/v15051163.
3. Encephalitic alphaviruses. Zacks MA, Paessler S. *Vet Microbiol*. 2010 Jan 27;140(3-4):281-6. doi: 10.1016/j.vetmic.2009.08.023. Epub 2009 Aug 28. PMID: 19775836
4. Current Understanding of the Molecular Basis of Venezuelan Equine Encephalitis Virus Pathogenesis and Vaccine Development. Sharma A, Knollmann-Ritschel B. *Viruses*. 2019 Feb 18;11(2):164. doi: 10.3390/v11020164.
5. Comparison of Aerosol- and Percutaneous-acquired Venezuelan Equine Encephalitis in Humans and Nonhuman Primates for Suitability in Predicting Clinical Efficacy under the Animal Rule. Rusnak JM, Dupuy LC, Niemuth NA, Glenn AM, Ward LA. *Comp Med*. 2018 Oct 1;68(5):380-395. doi: 10.30802/AALAS-CM-18-000027. Epub 2018 Oct 3.
6. Sequelae and Animal Modeling of Encephalitic Alphavirus Infections. Reyna RA, Weaver SC. *Viruses*. 2023 Jan 28;15(2):382. doi: 10.3390/v15020382.
7. Neurological Sequelae Resulting from Encephalitic Alphavirus Infection. Ronca SE, Dineley KT, Paessler S. *Front Microbiol*. 2016 Jun 20;7:959. doi: 10.3389/fmicb.2016.00959. eCollection 2016.
8. Taylor, K., Kolokoltsova, O., Ronca, S. E., Estes, M., & Paessler, S. (2017). Live, attenuated Venezuelan equine encephalitis virus vaccine (TC83) causes persistent brain infection in mice with non-functional $\alpha\beta$ T-cells. *Frontiers in Microbiology*, 8. <https://doi.org/10.3389/fmicb.2017.00081>
9. Characterization of Brain Inflammation, Apoptosis, Hypoxia, Blood-Brain Barrier Integrity and Metabolism in Venezuelan Equine Encephalitis Virus (VEEV TC-83) Exposed Mice by In Vivo Positron Emission Tomography Imaging. Bocan TM, Stafford RG, Brown JL, Akuoku Frimpong J, Basuli F, Hollidge BS, Zhang X, Raju N, Swenson RE, Smith DR. *Viruses*. 2019 Nov 13;11(11):1052. doi: 10.3390/v11111052.
10. Encephalitic Alphaviruses Exploit Caveola-Mediated Transcytosis at the Blood-Brain Barrier for Central Nervous System Entry. Salimi H, Cain MD, Jiang X, Roth RA, Beatty WL, Sun C, Klimstra WB, Hou J, Klein RS. *mBio*. 2020 Feb 11;11(1):e02731-19. doi: 10.1128/mBio.02731-19.
11. Virus entry and replication in the brain precedes blood-brain barrier disruption during intranasal alphavirus infection. Cain MD, Salimi H, Gong Y, Yang L, Hamilton

- SL, Heffernan JR, Hou J, Miller MJ, Klein RS. *J Neuroimmunol*. 2017 Jul 15;308:118-130. doi: 10.1016/j.jneuroim.2017.04.008. Epub 2017 May 1.
12. Toll-like receptor 4 mediates blood-brain barrier permeability and disease in C3H mice during Venezuelan equine encephalitis virus infection. Hollidge BS, Cohen CA, Akuoku Frimpong J, Badger CV, Dye JM, Schmaljohn CS. *Virulence*. 2021 Dec;12(1):430-443. doi: 10.1080/21505594.2020.1870834.
 13. Application of a Human Blood Brain Barrier Organ-on-a-Chip Model to Evaluate Small Molecule Effectiveness against Venezuelan Equine Encephalitis Virus. Boghdeh NA, Risner KH, Barrera MD, Britt CM, Schaffer DK, Alem F, Brown JA, Wikswo JP, Narayanan A. *Viruses*. 2022 Dec 15;14(12):2799. doi: 10.3390/v14122799.
 14. Blanchette M. & Daneman R. (2015). "Formation and maintenance of the BBB." *Science Direct. Mechanisms of Development*. Volume 138, Part 1. Pages 8-16. 26 Jul 2017. ISSN 0925-4773. <https://doi.org/10.1016/j.mod.2015.07.007>.
 15. Haddad-Tóvolli, R., Dragano, N. R. V., Ramalho, A. F. S., & Velloso, L. A. (2017). "Development and function of the blood-brain barrier in the context of metabolic control." *Frontiers in Neuroscience*, 11. <https://doi.org/10.3389/fnins.2017.00224>
 16. Inhibitors of Venezuelan Equine Encephalitis Virus Identified Based on Host Interaction Partners of Viral Non-Structural Protein 3. Bakovic A, Bhalla N, Alem F, Campbell C, Zhou W, Narayanan A. *Viruses*. 2021 Aug 3;13(8):1533. doi: 10.3390/v13081533.
 17. New World alphavirus protein interactomes from a therapeutic perspective. Carey BD, Bakovic A, Callahan V, Narayanan A, Kehn-Hall K. *Antiviral Res*. 2019 Mar;163:125-139. doi: 10.1016/j.antiviral.2019.01.015. Epub 2019 Jan 26.
 18. Anticancer pan-ErbB inhibitors reduce inflammation and tissue injury and exert broad-spectrum antiviral effects. Saul S, Karim M, Ghita L, Huang PT, Chiu W, Durán V, Lo CW, Kumar S, Bhalla N, Leyssen P, Alem F, Boghdeh NA, Tran DH, Cohen CA, Brown JA, Huie KE, Tindle C, Sibai M, Ye C, Khalil AM, Chiem K, Martinez-Sobrido L, Dye JM, Pinsky BA, Ghosh P, Das S, Solow-Cordero DE, Jin J, Wikswo JP, Jochmans D, Neyts J, De Jonghe S, Narayanan A, Einav S. *J Clin Invest*. 2023 Oct 2;133(19):e169510. doi: 10.1172/JCI169510.
 19. Inhibition of Venezuelan Equine Encephalitis Virus Using Small Interfering RNAs. Haikerwal A, Barrera MD, Bhalla N, Zhou W, Boghdeh N, Anderson C, Alem F, Narayanan A. *Viruses*. 2022 Jul 26;14(8):1628. doi: 10.3390/v14081628.
 20. Human cathelicidin peptide LL-37 as a therapeutic antiviral targeting Venezuelan equine encephalitis virus infections. Ahmed A, Siman-Tov G, Keck F, Kortchak S, Bakovic A, Risner K, Lu TK, Bhalla N, de la Fuente-Nunez C, Narayanan A. *Antiviral Res*. 2019 Apr;164:61-69. doi: 10.1016/j.antiviral.2019.02.002. Epub 2019 Feb 8.
 21. Efficacy of FDA-Approved Anti-Inflammatory Drugs Against Venezuelan Equine Encephalitis Virus Infection. Risner K, Ahmed A, Bakovic A, Kortchak S, Bhalla N, Narayanan A. *Viruses*. 2019 Dec 12;11(12):1151. doi: 10.3390/v11121151.
 22. Bivalent single domain antibody constructs for effective neutralization of Venezuelan equine encephalitis. Liu JL, Zabetakis D, Gardner CL, Burke CW, Glass PJ,

- Webb EM, Shriver-Lake LC, Anderson GP, Weger-Lucarelli J, Goldman ER. *Sci Rep.* 2022 Jan 13;12(1):700. doi: 10.1038/s41598-021-04434-x.
23. Kemp, Adrian. "Grants Saracatinib Orphan Drug Designation for Idiopathic Pulmonary Fibrosis" US FDA. AstraZeneca, 18 Mar. 2019, www.astrazeneca.com/media-centre/press-releases/2019/us-fda-grants-saracatinib-orphan-drug-designation-for-idiopathic-pulmonary-fibrosis-18032019.html.
 24. Synthetic Host Defense Peptides Inhibit Venezuelan Equine Encephalitis Virus Replication and the Associated Inflammatory Response. Ahmed A, Bakovic A, Risner K, Kortchak S, Der Torossian Torres M, de la Fuente-Nunez C, Lu T, Bhalla N, Narayanan A. *Sci Rep.* 2020 Dec 8;10(1):21491. doi: 10.1038/s41598-020-77990-3.
 25. Expression of the Antimicrobial Peptide Piscidin 1 and Neuropeptides in Fish Gill and Skin: A Potential Participation in Neuro-Immune Interaction. Zaccone G, Capillo G, Fernandes JMO, Kiron V, Lauriano ER, Alesci A, Lo Cascio P, Guerrero MC, Kuciel M, Zuwala K, Icardo JM, Ishimatsu A, Murata R, Amagai T, Germanà A, Aragona M. *Mar Drugs.* 2022 Feb 17;20(2):145. doi: 10.3390/md20020145.
 26. Structure-activity relationships of piscidin 4, a piscine antimicrobial peptide. Park NG, Silphaduang U, Moon HS, Seo JK, Corrales J, Noga EJ. *Biochemistry.* 2011 Apr 26;50(16):3288-99. doi: 10.1021/bi101395j. Epub 2011 Mar 31.
 27. Antimicrobial peptides from fish. Masso-Silva JA, Diamond G. *Pharmaceuticals (Basel).* 2014 Mar 3;7(3):265-310. doi: 10.3390/ph7030265.
 28. Use of tilapia piscidin 3 (TP3) to protect against MRSA infection in mice with skin injuries. Huang HN, Chan YL, Hui CF, Wu JL, Wu CJ, Chen JY. *Oncotarget.* 2015 May 30;6(15):12955-69. doi: 10.18632/oncotarget.4102.
 29. Host Defense Peptide Piscidin and Yeast-Derived Glycolipid Exhibit Synergistic Antimicrobial Action through Concerted Interactions with Membranes. Liu F, Greenwood AI, Xiong Y, Miceli RT, Fu R, Anderson KW, McCallum SA, Mihailescu M, Gross R, Cotten ML. *JACS Au.* 2023 Oct 19;3(12):3345-3365. doi: 10.1021/jacsau.3c00506. eCollection 2023 Dec 25.
 30. Nuclease activity gives an edge to host-defense peptide piscidin 3 over piscidin 1, rendering it more effective against persisters and biofilms. Libardo MDJ, Bahar AA, Ma B, Fu R, McCormick LE, Zhao J, McCallum SA, Nussinov R, Ren D, Angeles-Boza AM, Cotten ML. *FEBS J.* 2017 Nov;284(21):3662-3683. doi: 10.1111/febs.14263. Epub 2017 Sep 30.

BIOGRAPHY

Leykie I. Green graduated from Hampton High School, Hampton, Virginia, in 2018. She received her Bachelor of Science from James Madison University in Spring 2022 while performing research with an associate professor in Microbial Biomanufacturing of Nanobodies Projects. She then went on to start her Master of Science at George Mason University in Fall 2022.